Fire Technology, 52, 1051–1067, 2016

DOI: 10.1007/s10694-015-0520-z

Ignition of Wood Fencing Assemblies Exposed to Continuous Wind-Driven Firebrand Showers

Sayaka Suzuki, National Research Institute of Fire and Disaster (NRIFD), Chofu, Tokyo 182-8508, Japan

Erik Johnsson, Alexander Maranghides and Samuel L. Manzello, Fire Research Division, National Institute of Standards and Technology (NIST), Gaithersburg, MD 20899, USA*

Received: 8 April 2015/**Accepted:** 15 July 2015

Abstract. Post-fire studies conducted by NIST on the Waldo Canyon Fire in Colorado (2012) determined that wood fencing assemblies are believed to be vulnerable to ignition from firebrand showers in Wildland–Urban Interface fires, but again there has never been any experimental verification of this ignition mechanism. As a result, a series of experiments were conducted to examine ignition of wood fencing assemblies subjected to continuous, wind-driven firebrand showers. Western Red Cedar and Redwood fencing assemblies were exposed to continuous, wind-driven firebrands generated by the NIST full-scale Continuous Feed Firebrand Generator installed in the Fire Research Wind Tunnel Facility at the Building Research Institute in Japan. To simulate fine fuels that may be present near fencing assemblies, dried shredded hardwood mulch beds were placed adjacent to the fencing assemblies. The fencing assemblies were varied in length and in orientation to the applied wind field to simulate a range of configurations that may be encountered in realistic situations. Both flat and corner sections of fencing assemblies were used in these experiments. The dimensions of the flat wood fencing assemblies sections were varied from 0.91 m wide, 1.83 m in height to 1.83 m wide, 1.83 m in height. With respect to the corner sections, the dimensions used were 0.91 m by 0.91 m by 1.83 m in height. All configurations considered resulted in flaming ignition (FI) of the mulch beds, and subsequent FI of the wood fencing assemblies. Finally, experiments were also completed to determine if wind-driven firebrand showers could produce FI of fencing assemblies without the presence of fine fuels adjacent to the fence sections. Firebrands produced smoldering ignition (SI) of the fencing assemblies without fine fuels present, and SI transitioned to FI under the applied wind field. These experiments have demonstrated that wood fencing assemblies are vulnerable to ignition by wind-driven firebrand showers.

Keywords: WUI fires, Ignition, Firebrands

* Correspondence should be addressed to: Samuel L. Manzello, E-mail: samuelm@nist.gov

1. Introduction

Wildfires that spread into communities, referred to as Wildland–Urban Interface (WUI) fires, have destroyed communities throughout the world. WUI fires continue to burn in the USA, and are rapidly getting worse, with attendant increased economic costs [5]. Some recent examples include the Bastrop Complex Fire in Texas in 2011, the Waldo Canyon Fire in Colorado in 2012, and fires in Arizona, Colorado, and California in 2013.

Historically, fire safety science research has spent a great deal of effort to understand fire dynamics within buildings. Research into WUI fires, and how to potentially mitigate the loss of structures in such fires, is far behind other areas of fire safety science research. This is due to the fact that fire spread in the WUI is incredibly complex, involving the interaction of topography, weather, vegetation, and structures [17]. Interestingly, post-fire damage studies have suggested for some time that firebrands are a significant cause of structure ignition in WUI fires, yet for decades, firebrand studies have focused on understanding how far firebrands fly [1–3, 6, 7, 23, 29–33]. This understanding has not enabled the necessary hardening of structures in WUI communities. Experimental firebrand investigations have not been able to quantify the vulnerabilities of structures to ignition from firebrand showers, as it is difficult to develop a measurement method to replicate wind-driven firebrand exposure on structures that occur in actual WUI fire events.

To address this problem, research has been undertaken in an intricate area involving the quantification of structure vulnerabilities to wind-driven firebrand showers. This type of firebrand research has never been possible prior to the development of the NIST Firebrand Generator (Dragon). The NIST Dragon, coupled to a full-scale wind tunnel facility (Building Research Institute's in Japan), has begun to identify vulnerabilities of structures to wind-driven firebrand showers. The interested reader is directed elsewhere for recent comprehensive reviews of the NIST Dragon technology [14, 16, 18].

Post-fire studies conducted by NIST on the Waldo Canyon Fire in Colorado (2012) determined that wood fencing assemblies are believed to be vulnerable to ignition from firebrand showers in WUI fires [21], but again there has never been any experimental verification of this ignition mechanism. Figure 1 is picture of an ignited wood fencing assembly during a fire in CO.

To the authors' knowledge, the only available literature related to ignition of wood fencing assemblies to WUI fire exposures was studied in Australia [8]. In this work, various experiments with different fencing assemblies, such as wood fencing assemblies and steel fencing assemblies, were performed in both small-scale and large-scale experiments, in order to investigate the performance of residential boundary fencing systems. One of the large-scale experiments was intended to focus on attack from burning firebrands or leaf litter although no method was used to direct firebrand showers on the assemblies. Rather only leaf litter was used to simulate this scenario. Leaf litter was placed along the base of the inside of the fencing assemblies and ignited using a portable propane burner. Two kinds of wood assemblies were observed by this ignition method. Even though they attempted to simulate the ignition of the fencing assemblies in WUI fires, this

Figure 1. An ignited wood fencing assembly in Colorado, 2012; Courtesy of Colorado Springs Fire Department.

method is not a verification of the ignition mechanism by firebrands, as there was no dynamic wind-driven firebrand showers directed at the fencing assemblies.

To this end, Western Red Cedar and Redwood fencing assemblies were exposed to continuous, wind-driven firebrands generated by the NIST full-scale Continuous Feed Firebrand Generator (also known as the NIST full-scale Continuous Feed Dragon) installed in the Fire Research Wind Tunnel Facility (FRWTF) at the Building Research Institute (BRI) in Japan. To simulate fine fuels that may be present near fencing assemblies, dried shredded hardwood mulch beds were placed adjacent to fencing assemblies. The fencing assemblies were varied in length and in orientation to the applied wind field to simulate a range of configurations that would be encountered in realistic situations. Experiments were also completed to determine if wind-driven firebrand showers could produce flaming ignition (FI) of fencing assemblies without the presence of fine fuels adjacent to the fence sections. This work will inform test method development for a new generation of effective WUI building codes and standards, since the best way forward to address the WUI fire problem is hardening of structures [22, 25].

2. Experimental Description

Figure 2 is a schematic of the full-scale Continuous Feed Firebrand Generator. The description below closely follows descriptions available elsewhere but is repeated for completeness [16, 19, 28]. It is important to note that this device was recently used to expose decking assemblies, as well as mulch beds attached to non-combustible re-entrant corner assemblies, to continuous wind-driven firebrand showers [19, 28]. This version of the device was modified from the NIST Dragon [9–13, 15] and consisted of two parts: the main body and continuous feeding com-

ponent. The feeding system was connected to the main body and was equipped with two gates to prevent fire spread (described in more detail below). Each gate was alternatively opened and closed. A blower was connected to the main body and the purpose of the blower is described below. All components of the full-scale Continuous Feed Firebrand Generator were constructed of stainless steel. A major challenge when constructing this device was designing a completely contained feeding system shielded from the wind tunnel flow.

The feeding system consisted of a pneumatic cylinder coupled to a cylindrical container where wood pieces were stored (see Figure 2). The pneumatic cylinder was contained inside a metal sleeve. Inside the metal sleeve, the sliding rod of the pneumatic cylinder was connected to a plate that allowed the volume of wood contained within the sleeve to be varied. This volume was set precisely to allow a specific mass of firebrands to fall into this volume. When the air pressure was applied, the sliding rod of the pneumatic cylinder moved forward and forced the wood pieces within the volume of the metal sleeve to the first gate, where they were then dropped into the second gate that leads to the Dragon where they are ignited (see Figure 2). Care was taken to select the pneumatic cylinder (15 cm bore with 15 cm stroke; maximum pressure of 1.7 MPa and maximum load of 31 kN); smaller sized pneumatic cylinders were observed to be unable to force the wood pieces to the first gate and would jam. The gate system was required to contain the fire from spreading from the Dragon to the feed system and each gate was driven by pneumatic cylinders as well. For all tests, Douglas-fir wood pieces machined to dimensions of 7.9 mm (H) by 7.9 mm (W) by 12.7 mm (L) were used to produce firebrands (see Figure 3). The same-sized wood pieces were used to

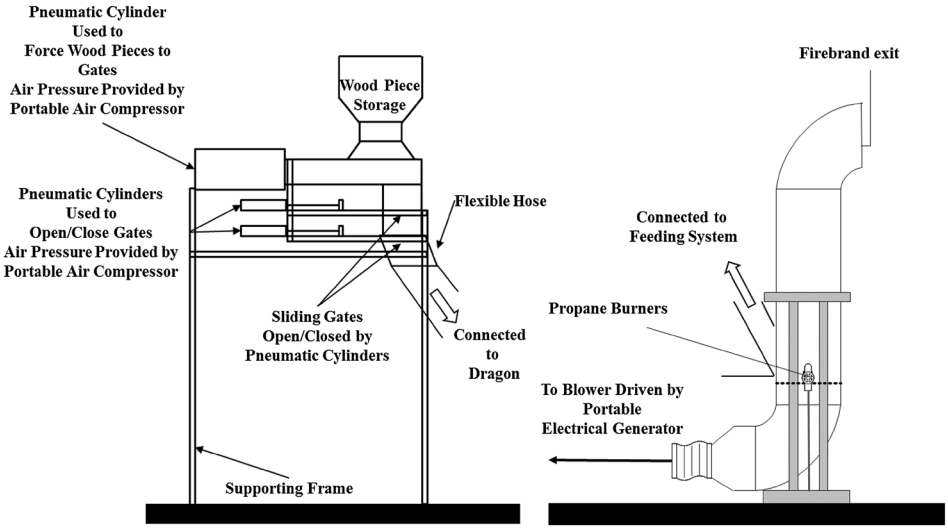

Figure 2. Side view of the main body (or Dragon) of the full-scale Continuous Feed Firebrand Generator. The feeding system that provided wood pieces into the device is shown.

feed the bench-scale continuous Firebrand Generator in past studies and have been shown to be commensurate with sizes measured from full-scale burning trees, as well as size distributions obtained from actual WUI fires [10, 20].

An operational parameter that was varied was the blower speed. When the blower was set to provide an average velocity below 3 m/s measured at the exit of the Dragon when no wood pieces were loaded, insufficient air was supplied for combustion and this resulted in a great deal of smoke being generated in addition to firebrands. At blower velocities above 3 m/s, smoke production was mitigated, but many firebrands produced were in a state of flaming combustion as opposed to glowing combustion. It has been suggested that firebrands fall at or near their terminal settling velocity. As such, when firebrands contact ignitable fuel beds, they are most likely in a state of glowing combustion, not open flaming [29]. It is possible for firebrands to remain in a flaming state under an air flow and, it is reasonable to assume that some firebrands may still be in a state of flaming combustion upon impact. The purpose of this device was to simulate firebrand showers observed in long-range spotting, and therefore, glowing firebrands were desired.

As in prior experiments using the NIST Dragon, the new experimental device was installed inside BRI's FRWTF (see Figure 4). The facility was equipped with a 4 m diameter fan to produce the wind field. The cross section of the FRWTF is 5 m wide by 4 m high. The experimental device was installed inside the test section of the FRWTF.

The wood fencing assemblies were placed at a distance of 3.25 m downstream of the full-scale Continuous Feed Firebrand Generator (see Figure 4). Assemblies located at this distance are known to receive an intense flux of firebrands from the Dragon [19, 28]. Both flat and corner sections of fencing assemblies were used in these experiments. The dimensions of the flat wood fencing assemblies sections were varied from 0.91 m (3 ft) wide, 1.83 m (6 ft) in height to 1.83 m (6 ft) wide, 1.83 m (6 ft) in height. With respect to the corner sections, the dimensions used were 0.91 m (3 ft) by 0.91 m (3 ft) by 1.83 m (6 ft) in height.

To simulate fine fuels that may be present near fencing assemblies, dried shredded hardwood mulch beds were placed adjacent to the fencing assemblies. It was

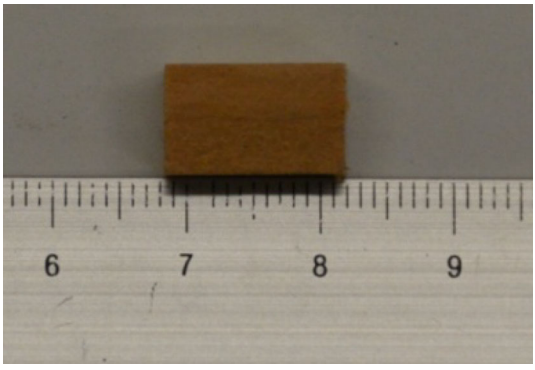

Figure 3. Single wood piece, ruler primary units are in centimeters.

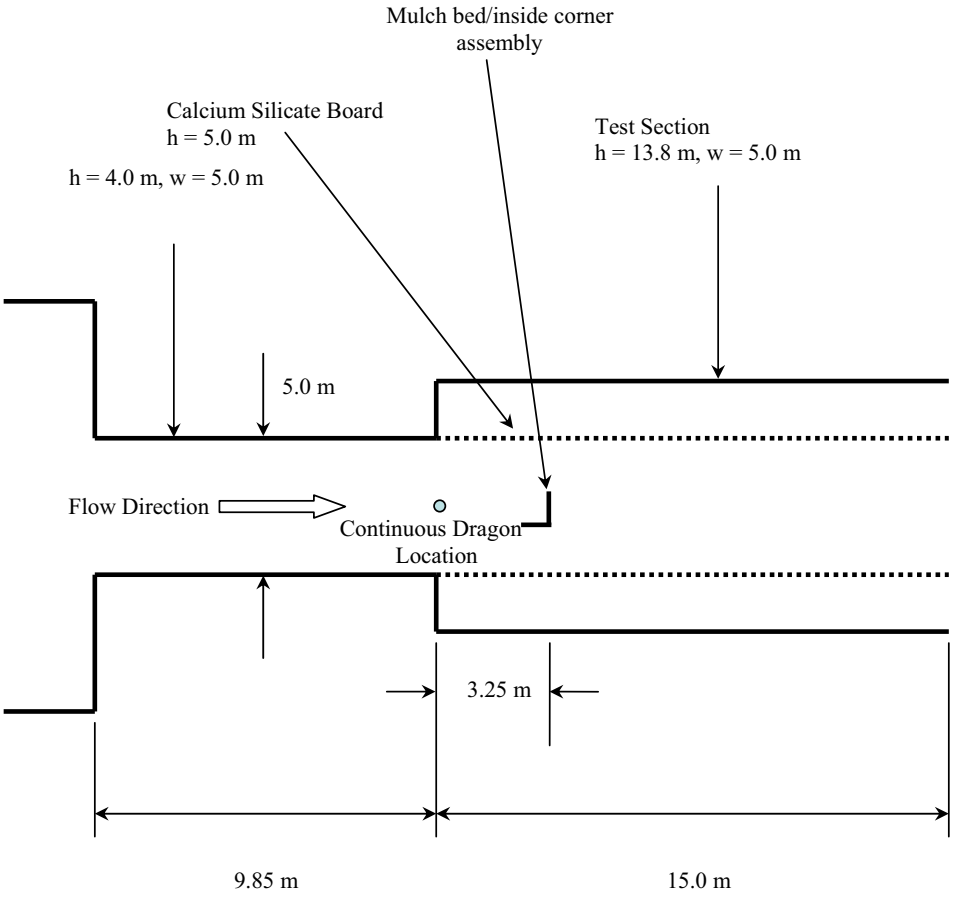

Figure 4. Schematic of BRI's FRWTF. The locations of the full-scale Continuous Feed Firebrand Generator and the wood fencing assemblies are shown.

speculated that fine fuels would easily be ignited by wind-driven firebrand showers, and the subsequent ignition of the fine fuel may lead to fence ignition. Shredded hardwood mulch was selected as a surrogate for fine fuels that may be encountered in WUI areas. The mulch bed thickness was fixed at 51 mm; a commonly recommended mulch thickness [4]. The mulch bed density was 0.3 g/cm^3. The overall dimensions of the mulch beds were varied in order to maintain the same mulch bed density in each experiment. To simulate a worse-case scenario, the shredded hardwood mulch was oven dried in all experiments. Another experimental series was also completed to determine if wind-driven firebrand showers could produce FI of fencing assemblies without the presence of fine fuels adjacent to the fence sections.

For completeness, Figure 5 displays a drawing of the various configurations considered, and Table 1 provides a summary of the experimental conditions. Each configuration is explained in detail below. The fencing assemblies were varied in

Table 1
Experimental Conditions

Mulch condition	Configuration		Material	Wind speed (m/s)
Dried mulch	0.91 m wide flat wall assembly	a	Cedar	8
Dried mulch	Inside corner assembly	b	Cedar	8
Dried mulch	Inside corner assembly	b	Redwood	8
Dried mulch	Outside corner assembly	c	Cedar	8
Dried mulch	1.83 m wide flat wall assembly	d	Cedar	8
No mulch	0.91 m wide flat wall assembly	e	Cedar	8
No mulch	Inside corner assembly	f	Cedar	8
No mulch	V-corner assembly	g	Cedar	8

Mulch condition (dried mulch or no mulch), the configuration, and the material (cedar or redwood) were changed. Each configuration used is shown in Figure 5

orientation to the applied wind field to simulate a range of configurations that may be encountered in realistic situations. Most of the fencing assemblies were made from Western Red Cedar; one of the assemblies was made from Redwood in order to observe the effect of fencing material.

A typical experiment was conducted in the following manner. The wood fencing assembly to be experimented on was installed inside the test section of the FRWTF. The wind tunnel speed was set to the desired level (e.g. 8 m/s). Wood pieces were first loaded into the cylinder storage container, and the air compressor needed to provide compressed air for the pneumatic cylinder and gate system was switched on (air compressor pressure was set to 0.7 MPa). The blower was set at 3 m/s, and two propane burners were ignited and inserted into the side of the device. The propane burners were operated continuously during the experiment. The pneumatic piston was then activated and the sliding rod was positioned to allow wood pieces to enter the volume in the metal sleeve. The sliding rod was moved to push the wood pieces (200 g) to the first gate. The gate was opened, closed, and the second gate was then opened, and the wood fell into the Dragon. The feeding was varied to determine the optimal conditions for continuous firebrand showers. It was observed that 200 g, fed into the Dragon every 15 s provided an adequate firebrand generation rate to ignite building materials. A supply of 200 g corresponded to approximately 400 wood pieces deposited every 15 s.

3. Results and Discussion

3.1. Number/Mass Flux of Generated Firebrands from the Full-Scale Continuous Feed Firebrand Generator

The number flux (number of firebrands generated/m^2s), at the exit of the device, was measured at a feeding rate of 200 g every 15 s (800 g/min). To determine the number flux, the number of firebrands was counted at every frame of the video recording, summed every second, and then summed again at every ten seconds. Based on the analysis, the number flux reached a steady value of 342.0/m^2s 300 s

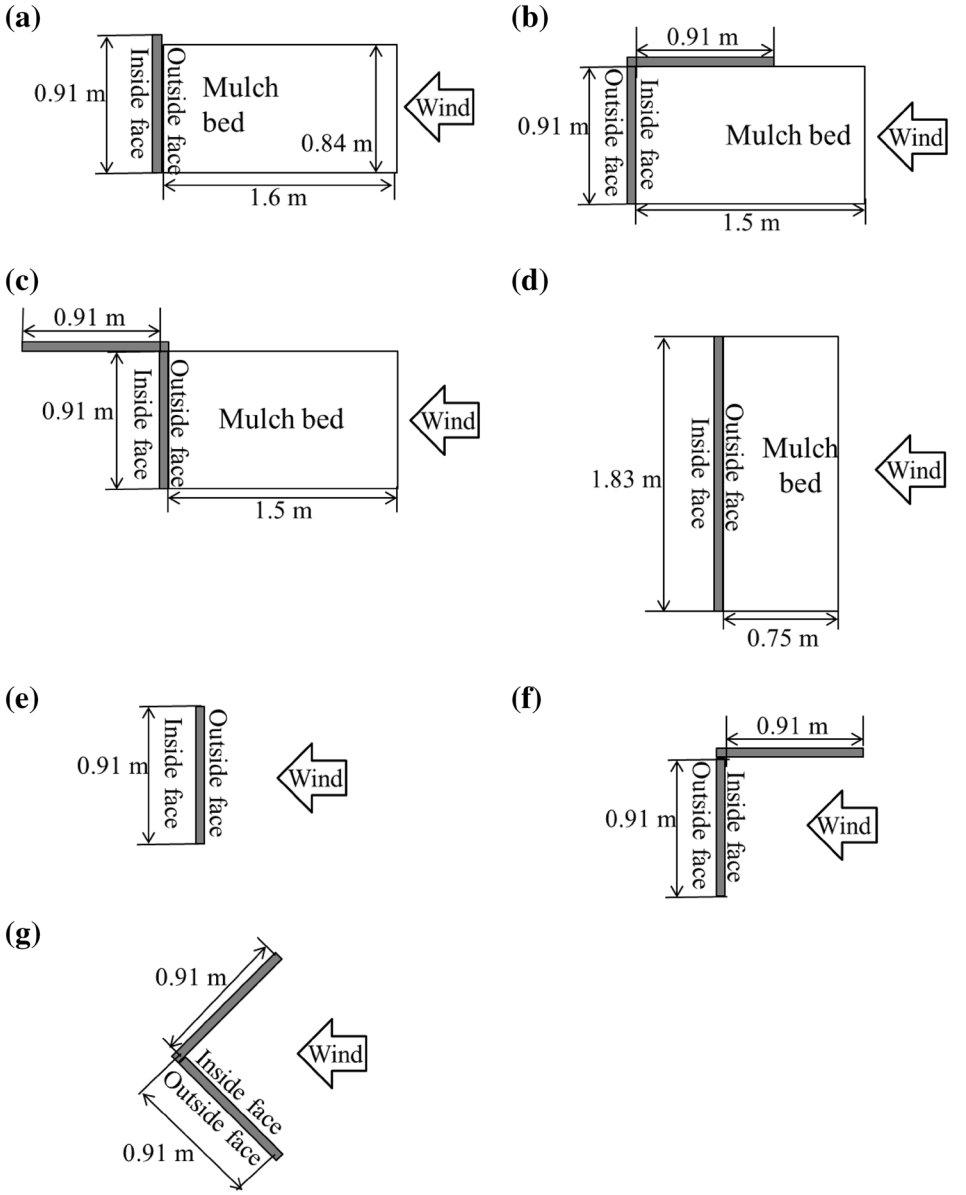

Figure 5. The configurations of experiments performed in this study. Wood fencing assemblies placed *adjacent to fine fuels* (a) 0.91 m wide flat wall assembly, (b) inside corner assembly, (c) outside corner assembly, (d) 1.83 m wide flat wall assembly. Wood fencing assemblies without *adjacent fine fuels*, (e) 0.91 m wide flat wall assembly, (f) inside corner assembly, (g) V-corner assembly.

after feeding began. The first firebrands began to be generated ~100 s after feeding was commenced.

Mass flux data (mass of firebrands generated/m^2s) were calculated by multiplying the number flux and the average mass of each firebrand at a feed rate of 200 g every 15 s. To measure the firebrand mass, another set of experiments was conducted using a series of water pans were placed downstream of the NIST full-scale Continuous Feed Firebrand Generator. Water pans were required in order to quench combustion of the firebrands. If the water pans were not used, the firebrands would continue to burn and by the time collection was completed; only ash would remain. After the experiment was finished, the pans were collected and the firebrands were filtered from the water, using a series of fine-mesh filters. Firebrands were dried in an oven, at 104°C, for 16 h. As in previous work, the mass versus drying time was monitored to determine the duration needed to completely dry the firebrands. The mass and dimension of each firebrand were measured using precision calipers (1/100 mm resolution) and a precision balance (0.001 g resolution). Figure 6 displays the projected area of the generated firebrands at 8 m/s. Image analysis software was used to determine the projected area of a firebrand by converting the pixel area using an appropriate scale factor. It was assumed that deposited firebrands would rest flat on the ground and the projected areas with the maximum dimension and the second maximum dimension of three dimensions were measured (for cylindrical and flat shaped firebrands respectively). Images of well-defined shapes (e.g. circular objects) were used to determine the ability of the image analysis method to calculate the projected area (Suzuki et al. [27]. Based on repeat measurements of different areas, the standard uncertainty in determining the projected area was ±10%. The mass of each firebrand was mea-

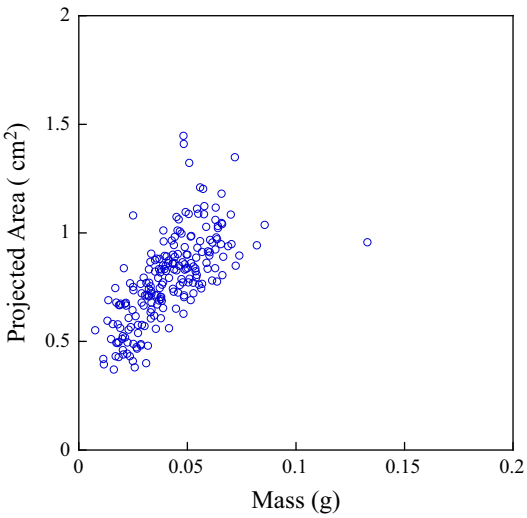

Figure 6. Projected area of generated firebrands as a function of mass at 8 m/s.

sured by a precision balance with 0.001 g resolution. Repeat measurements of known calibration masses were measured by the balance which was used for the firebrand mass analysis. The standard uncertainty in the firebrand mass was approximately ±1%. The mean mass and standard deviation of each firebrand were obtained and observed to be 0.05 g ± 0.02 g. Therefore, the mass flux of generated firebrands was calculated to be 17.1 g/m^{2}s.

An important characteristic of the NIST Dragon is that the firebrand size and mass produced using the device can be tailored to those measured from full-scale tree burns [10], and actual WUI fires [20]. In collaboration with the California Department of Forestry and Fire Protection (CALFIRE), NIST quantified firebrand distributions from a real WUI fire (2007 Angora Fire) for the first time [20]. Specifically, digital image analyses of burn patterns from materials exposed to the Angora Fire were conducted to determine firebrand size distributions. The most salient result reported in Manzello and Foote [20] was the documentation of the consistently small size of firebrands (<0.5 cm^2) and the close correlation of these results with the sizes of experimentally generated firebrands from the NIST Dragon. The Texas Forest Service has used this methodology to collect firebrand size distributions from the recent Texas Bastrop Complex fires in 2011, as well, and reported similar findings to the 2007 Angora fire; significant numbers of very small firebrands were produced [26].

3.2. *Wood Fencing Assemblies Located Adjacent to Fine Fuels*

Wind-driven firebrand showers were directed at various configurations of the wood fencing assemblies placed adjacent to fine fuels, and these are shown in Figure 5a–d. To provide clarity to the discussion, the configurations of the fencing assemblies are labeled as, (a) 0.91 m wide flat assembly, (b) inside corner assembly, (c) outside corner assembly, and (d) 1.83 m wide flat assembly, respectively. For the fencing assemblies, the side with the lateral bracing is intended to face the inside of the fenced area, thus inside face in Figure 5 denotes the side with the lateral bracing. Outside face refers to the smooth side of the fencing assembly.

In all experiments in which fine fuels were placed adjacent to fencing assemblies, the following ignition process was observed. Several glowing firebrands accumulated on the mulch beds near the fencing assemblies. This accumulation of firebrands produced smoldering ignition (SI) in the mulch beds that transitioned to FI of the mulch beds. The FI of the mulch bed eventually produced FI of the fencing assemblies. All FI of the fencing assemblies were sustainable. An image of FI of the fencing assemblies is shown in Figure 7. The time to reach FI of the fencing assemblies, ignited by the fine fuels, is shown in Table 2. It is interesting to observe that all the fencing assemblies were ignited within 30 s after the mulch beds were ignited, regardless of the configuration or wood fencing assembly type. Figure 7 also shows that ignited fencing assembly produced their own large firebrands. The fencing assembly made from Redwood, compared to those from Western Red Cedar, was observed to produce larger firebrands during the combustion process. This result is important as it demonstrates that ignited wood fencing may

also produce additional firebrand showers. More experiments are required to better quantify the firebrand production process from ignited fencing assemblies.

The numbers of firebrands that landed on the mulch beds were measured for each configuration, and are shown in Table 3. Based on this analysis, the numbers of firebrands that landed on the mulch beds per second (after the firebrand production from Dragon was stabilized) were 14/s, 13/s, 11/s, and 8/s for the inside corner assembly, outside corner assembly, 0.91 m wide flat wall assembly, and 1.83 m wide flat wall assembly, respectively. The area of all the mulch beds in this experimental series was kept at 1.39 m^2, (15 ft^2). The ratio (%) of the numbers of firebrands that landed on the mulch beds to the numbers of firebrands produced from the Dragon's outlet were 56%, 53%, 45%, and 33% for the inside corner assembly, outside corner assembly, 0.91 m wide flat assembly, and 1.83 m wide flat assembly, respectively. Clearly, the numbers of firebrands that landed on the

Table 2
Time to FI of the Fencing Assembly from FI of the Mulch Beds

Configuration		Material	Time to FI of the fencing assembly after FI of the mulch beds (s)
0.91 m wide flat wall assembly	a	Cedar	14
Inside corner assembly	b	Cedar	25
Inside corner assembly	b	Redwood	23
Outside corner assembly	c	Cedar	29
1.83 m wide flat wall assembly	d	Cedar	9

Figure 7. FI of the inside corner assembly (redwood, dimension shown Figure 5b) placed adjacent to fine fuels. In the figure, firebrands can be seen that are generated from the ignited fencing.

mulch beds were affected by the wind flow around the assemblies. As indicated, the areas of the mulch beds were kept the same in order to be able to maintain the same mulch bed density in each experiment. For the 1.83 wide flat wall assembly, this resulted in the mulch bed having the longest lateral dimension exposed to firebrand showers (0.45 m × 3.0 m). Regardless, it was observed that most of firebrands could not reach the mulch bed for this case; rather the firebrands landed far ahead from the assembly due to wind flow around the assembly. There is qualitative agreement with prior work that demonstrated that the nature of the obstacles in the flow influences the stagnation zones, and thus firebrand accumulation [13].

The time to reach sustained FI of the mulch beds from the time when the first firebrand landed on the mulch beds was measured and shown in Table 3. Clearly, the time to FI was affected by the number of firebrands that landed on the mulch beds per second. The time to FI decreased as more firebrands landed on the mulch beds per second.

The relationship between the time to FI and the total number of firebrands for FI is shown in Figure 8. Those experiments were performed under the same condition, such as the area of the mulch beds, the wind speed, the firebrand mass flux from Dragon and MC (dried) as described above. Figure 8 shows that the total number of firebrands required for FI for the 1.39 m^2 mulch bed is almost constant; 1010 firebrands with standard deviation of 150 firebrands. Such numbers of firebrands are not a significant amount of firebrands, and in actual WUI fires, may easily be produced.

3.3. Wood Fencing Assemblies: Without the Presence of Fine Fuels

Without the presence of fine fuels, the three different configurations tested are shown in Figure 5e–g; (e) 0.91 m wide flat wall assembly, (f) inside corner assembly, and (g) V-corner assembly. It is interesting to observe that all configurations shown here were ignited within 20 min by only firebrand showers. The results are summarized in Table 4. It was observed that these fencing assemblies possessed

Table 3
Time to FI of the Fencing Assembly from the Time When First Firebrand Landed on the Mulch Beds and the Number of Firebrands Landed on the Mulch Bed for Each Configuration

Configuration		Material	Time to FI of the much bed from the time when first firebrand landed on the mulch beds (s)	The number of firebrands that landed on the mulch beds (/s)
0.91 m wide flat wall assembly	a	Cedar	103	11
Inside corner assembly	b	Cedar	78	14
Inside corner assembly	b	Redwood	59	14
Outside corner assembly	c	Cedar	82	13
1.83 m wide flat wall assembly	d	Cedar	104	8

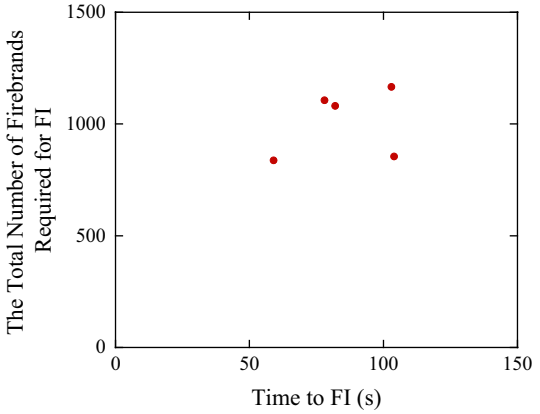

Figure 8. Relationship between time to FI and the total number of firebrand required for FI.

Table 4
Summary of Ignition Results of the Fencing Assemblies Without Mulch Beds by Firebrand Showers

Configuration		Ignition at the bottom	Ignition at the joints
0.91 m wide flat wall assembly	e	Ignited but not sustained	Ignited and sustained
Inside corner assembly	f	Ignited but not sustained	NA
V-corner assembly	g	Ignited but not sustained	Ignited and sustained

two different potential ignition vulnerabilities: the base (see Figure 9), and the joints of the lateral bracing and fencing boards (see Figure 9). The inside corner assembly and V-corner assembly had both of these vulnerabilities, whereas the 0.91 m wide flat assembly had only one potential ignitable point, the base, since the outside face, the side with no lateral bracings, faced the firebrand showers.

Firebrands accumulated at the base of the fencing assemblies and started to ignite with the heat from firebrand accumulation. The ignitions at the base were SI. Yet, these ignitions at the base were observed to be unsustainable. Holes were generated at the base of the assemblies from firebrand ignition and firebrands subsequently went through the burned holes and did not accumulate anymore at the base (see Figure 10).

The ignition of the fencing assembly at the joints of lateral bracing and fencing boards were also observed. A picture of FI of the fencing assembly is shown in Figure 11 (the experiment with the V-corner). Firebrands were trapped with the joints of lateral bracings, lateral bracing and the fencing boards, or inside edge of the corner assembly. This led to the SI. In this case, the SI was sustainable, which was different behavior from what was observed at the base. Firebrands remained at the joints of the lateral bracing and fencing boards for a longer time compared

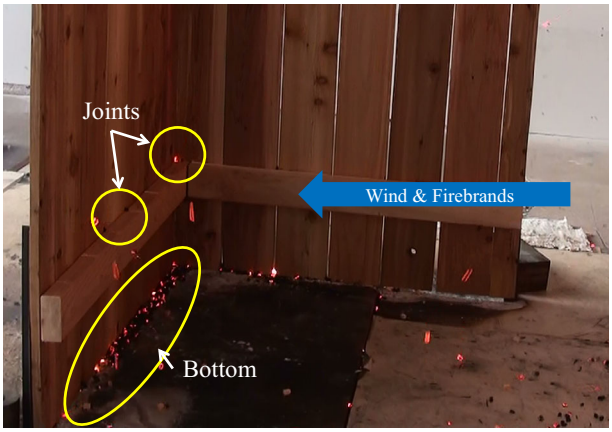

Figure 9. Two potential ignitable points of the wood fencing assemblies by firebrand showers are shown; one at the bottom and the other at the joints of the lateral bracings and the fencing boards.

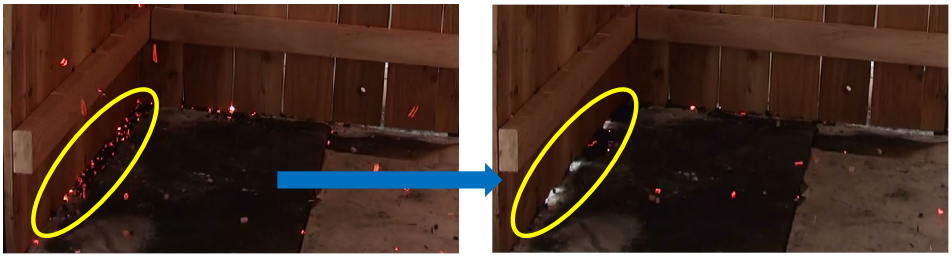

Figure 10. Bottom of the fencing assembly under firebrand attack. *Left* firebrands were accumulated at the bottom of the assembly. *Right* the assembly had a hole and firebrands were no longer accumulated, but went through.

to the base (see Figure 10 for base). The reason for this is less firebrands arrived at these locations, as compared to the base, and as a result, large holes were not produced quickly. In addition, the occasional transition from SI to FI was also observed. The transition from SI to FI requires a mixture of pyrolysis gases and air within the flammability limit and sufficient heat source to ignite at the same time [24]. Firebrands which remained within the joints kept providing the heat source to the joints in these experiments. The wood has to be arranged so that the heat loss can be minimal in order for the wood to transit from SI to FI [24]. In this study, firebrands remained trapped at the joints of lateral bracing and fencing boards, which it is thought to minimize the heat loss from firebrands themselves and encouraged the transition from SI to FI.

Figure 11. FI of the joints of V-corner assembly.

4. Conclusions

These experiments have demonstrated the wood fencing assemblies are vulnerable to ignition by wind-driven firebrand showers, even without the presence of fine fuels located adjacent to the assemblies. It was also observed that ignited fencing assembly produced their own large firebrands. The fencing assembly made from Redwood, compared to those from Western Red Cedar, was observed to produce larger firebrands during the combustion process. This result is important as it demonstrates that ignited wood fencing may also produce additional firebrand showers. More experiments are required to better quantify the firebrand production process from ignited fencing assemblies, as well as fire spread along these assemblies. Finally, additional experiments would be helpful to determine if ignited fencing assemblies can produce ignition of adjacent building elements.

Acknowledgments

The authors would like to acknowledge the many contributions from Mr. Edward Hnetkovsky, Mr. John Shields, Mr. Laurean DeLauter, Mr. Tony Chakalis, and Mrs. Doris Rinehart, all of the Engineering Laboratory (EL) at NIST. Dr. Matthew Bundy, NIST National Fire Research Laboratory (NFRL) Director, is acknowledged for making NFRL technicians available to support this work by preparing all materials for shipping to Japan. The Building Research Institute (BRI) is acknowledged for the use of the Fire Research Wind Tunnel Facility (FRWTF).

References

1. Albini F (1979) Spot fire distance from burning trees—a predictive model. USDA Forest Service, Intermountain Forest and Range Experiment Station, General Technical Report INT-56. Ogden, UT

2. Albini F (1983) Transport of firebrands by line thermals. Combust Sci Technol 32:277–288. doi:10.1080/00102208308923662
3. Anthenien R, Tse SD, Fernandez-Pello AC (2006) On the trajectories of embers initially elevated or lofted by small-scale ground fire plumes in high winds. Fire Saf J 41:349–363. doi:10.1016/J.FIRESAF.2006.01.005
4. Beyler C, Dinaburg J, Mealy C (2014) Development of test methods for assessing the fire hazards of landscape Mulch. Fire Technol 50:39–60. doi:10.1007/s10694-012-0264-y
5. Gorte R (2013) The rising cost of wildfire protection. Headwaters Econ. http://headwaterseconomics.org/wphw/wp-content/uploads/fire-costs-background-report.pdf
6. Himoto K, Tanaka T (2005) Transport of disk-shaped firebrands in a turbulent boundary layer. In: Gottuk DT, Lattimer BY (eds) Fire safety science—proceedings of the eighth symposium, 18–23 September 2005, Beijing, China, vol 8. International Association for Fire Safety Science, London, pp 433–444
7. Knight IK (2001) The design and construction of a vertical wind tunnel for the study of untethered firebrands in flight. Fire Technol 37:87–100. doi:10.1023/A:1011605719943
8. Leonard JE, Blanchi R, White N, Bicknell A, Sargeant A, Reisen F, Cheng M, Honavar K (2006) Research and investigation into the performance of residential boundary fencing systems in bushfires, CMIT-2006-186
9. Manzello SL, Shields JR, Yang JC, Hayashi Y, Nii D (2007) On the use of a firebrand generator to investigate the ignition of structures in wildland–urban interface (WUI) fires. In: 11th international conference on fire science and engineering (INTERFLAM), 3–5 September 2007, London, UK. Interscience Communications Ltd, London
10. Manzello SL, Maranghides A, Shields JR, Mell WE, Hayashi Y, Nii D (2009) Mass and size distribution of firebrands generated from burning Korean pine (Pinus koraiensis) trees. Fire Mater J 33:21–31
11. Manzello SL, Park SH, Shields JR, Hayashi Y, Suzuki S, (2010a) Comparison testing protocol for firebrand penetration through building vents: summary of BRI/NIST full scale and NIST reduced scale results, NIST TN 1659
12. Manzello SL, Hayashi Y, Yoneki Y, Yamamoto Y (2010) Quantifying the vulnerabilities of ceramic tile roofing assemblies to ignition during a firebrand attack. Fire Saf J 45:35–43
13. Manzello SL, Park SH, Shields JR, Suzuki S, Hayashi Y (2011) Experimental investigation of structure vulnerabilities to firebrand showers. Fire Saf J 46:568–578
14. Manzello SL, Suzuki S, Hayashi Y (2012) Enabling the study of structure vulnerabilities to ignition from wind driven firebrand showers: a summary of experimental results. Fire Saf J 54:181–196
15. Manzello SL, Suzuki S, Hayashi Y (2012) Exposing siding treatments, walls fitted with eaves, and glazing assemblies to firebrand showers. Fire Saf J 50:25–34
16. Manzello SL, Suzuki S (2013) Experimentally simulating wind driven firebrand showers in Wildland-Urban Interface (WUI) fires: overview of the NIST firebrand generator (NIST dragon) technology. Proced Eng 62:91–102
17. Manzello SL (2014) Special issue on Wildland-Urban Interface (WUI) fires. Fire Technol 50(1):7–8. doi:10.1007/s10694-012-0319-0
18. Manzello SL (2014b) Enabling the investigation of structure vulnerabilities to wind-driven firebrand showers in wildland-urban interface (WUI) fires. In: van Hees P, Jansson R, Nilsson D (eds) Fire safety science-proceedings of the eleventh international symposium on fire safety science, vol 11, IAFSS, (2014). (In print)
19. Manzello SL, Suzuki S (2014c) Exposing decking assemblies to continuous wind-driven firebrand showers. In: van Hees P, Jansson R, Nilsson D (eds) Fire safety science-pro-

ceedings of the eleventh international symposium on fire safety science, vol 11, IAFSS, (2014). (In print)
20. Manzello SL, Foote EID (2014) Characterizing firebrand exposure from Wildland-Urban Interface (WUI) fires: results from the 2007 Angora fire. Fire Technol 50(1):105–124. doi:10.1007/s10694-012-0295-4
21. Maranghides, A (2015) NIST study of Waldo Canyon Fire (in preparation)
22. Mell WE, Manzello SL, Maranghides A, Butry D, Rehm RG (2010) The Wildland-Urban Interface fire problem—current approaches and research needs. Int J Wildland Fire 19:238–251
23. Muraszew A, Fedele JF (1976) Statistical model for spot fire spread. The Aerospace Corporation Report Number ATR-77758801. Los Angeles, CA
24. Ohlemiller T (1991) Smoldering combustion propagation on solid wood. In: Cox G (ed) Fire safety science—proceedings of the third international symposium, vol 3. IAFSS, 565-574
25. Pellegrino JL, Bryner NP, Johnsson EL (2013) Wildland-urban Interface fire research needs—Workshop Summary Report, NIST SP 1150
26. Rissel S, Ridenour K (2013) Ember production during the Bastrop complex fire. Fire Manag Today 72:7–13
27. Suzuki S, Manzello SL, Lage M, Laing G (2012) Firebrand generation data obtained from a full-scale structure burn. Int J Wildland Fire 21:961–968
28. Suzuki S, Manzello SL, Kagiya K, Suzuki J, Hayashi Y (2015) Ignition of mulch beds exposed to continuous wind-driven firebrand showers. Fire Technol 51:905–922. doi:10.1007/s10694-014-0425-2
29. Tarifa CS, del Notario PP, Moreno FG (1965) On the flight paths and lifetimes of burning particles of wood. Proc Combust Inst 10:1021–1037
30. Tarifa CS, del Notario PP, Moreno FG (1967) Transport and combustion of fire brands. Instituto Nacional de Tecnica Aerospacial 'Esteban Terradas', Final Report of Grants FG-SP-114 and FG-SP-146, vol 2. Madrid, Spain
31. Tse SD, Fernandez-Pello AC (1998) On the flight paths of metal particles and embers generated by power lines in high winds and their potential to initiate wildfires. Fire Saf J 30:333–356. doi:10.1016/S0379-7112(97)00050-7
32. Wang HH (2011) Analysis on downwind distribution of firebrands sourced from a wildland fire. Fire Technol 47:321–340. doi:10.1007/S10694-009-0134-4
33. Woycheese JP (2000) Brand lofting and propagation for large-scale fires. PhD dissertation, University of California, Berkeley, CA